

Entropic Attraction and Repulsion in Binary Colloids Probed with a Line Optical Tweezer

J. C. Crocker, J. A. Matteo, A. D. Dinsmore,* and A. G. Yodh

Department of Physics and Astronomy, University of Pennsylvania, 209 S. 33rd Street, Philadelphia, Pennsylvania 19104
(Received 15 June 1998)

The long-range entropic forces that arise between two micrometer-sized colloidal spheres in a fluid of much smaller colloidal spheres were directly measured using a line-scanned optical tweezer. This new technique allowed us to measure the functional form of the potential with sub- $k_B T$ energy and 15 nm spatial resolution. At the lowest small sphere concentrations, the potential was monotonically attractive, while at higher concentrations an oscillatory potential was observed, due to the liquid structure of the small spheres. Surprisingly, the large spheres came together only rarely at the higher concentrations, suggesting a new means for stabilizing suspensions using entropy alone. [S0031-9007(99)09246-7]

PACS numbers: 82.70.Dd, 61.25.Hq

Entropic forces between macromolecules in suspension are often produced by the addition of smaller particles to the background solvent [1–11]. These forces have considerable technological importance ranging from protein crystallization to the reversible aggregation of industrial suspensions. At low concentrations of the small species, the forces are traditionally described by the depletion model of Asakura and Oosawa [1], which predicts a monotonically attractive potential, with a range given by the small species diameter. When the smaller particles are concentrated, however, their liquid-structural correlations can dramatically change the interaction to include a repulsive or even oscillatory component [3].

We present the first direct measurement of these effects between two colloidal particles in suspension. Our experiments reveal depletion attraction and repulsion, and exhibit an unexpected slowing down of the aggregation kinetics as the small spheres are made more concentrated. We measured the interaction potential between an isolated pair of 1100 ± 15 nm diameter PMMA (polymethylmethacrylate) spheres (Bangs Labs, Inc) induced by a background of smaller, 83 nm diameter PS (polystyrene) spheres (Seradyn, Inc). We varied the volume fraction of the small spheres, ϕ_S , by diluting the $\phi_S = 0.42$ stock solution (as measured by viscometry [12]) with a buffer of 5 mM NaCl and 5 mM SDS surfactant, which prevents colloidal aggregation. The bare interactions between the individual large or small spheres are expected to be a screened electrostatic repulsion [13] with a 3 nm screening length. Since this length is so small compared to the particle diameters, we can treat the bare interaction as effectively hard spherelike. However, this electrostatic repulsion does cause the small spheres' effective radius to be slightly larger than their actual radius [10].

The entropic interactions between a pair of the larger spheres were measured by threading the larger spheres on a rod of light, i.e., a line-scanned optical tweezer [14,15]. In this trap, colloidal spheres are free to diffuse in one dimension, along the scan direction, while being strongly confined in the two perpendicular directions. The

system's own thermal fluctuations then allow us to map out the pair interaction. Specifically, we trap two large spheres in the line tweezer and measure the probability of finding them at a given separation using digital video microscopy. The measured equilibrium probability $P(r)$ of finding the spheres with separation r is given by the Boltzmann equation, $P(r) \propto \exp[-F(r)/k_B T]$, where $F(r)$ is the system's Helmholtz free energy.

The measured large sphere pair potentials are presented in Fig. 1 for seven values of ϕ_S ranging from 0.04 to 0.42, as well as a control measurement with $\phi_S = 0$. The most prominent feature is a strong attraction at short range. An explanation of this attractive depletion force was first provided by the Asakura-Oosawa [1] (AO) theory, which assumes that the small spheres behave as an ideal gas. Around each large sphere there is a thin shell, or "depletion zone" (Fig. 2a), into which the centers of the small spheres cannot penetrate. When two large spheres approach each other, their depletion zones overlap, increasing the total volume accessible to the small spheres, increasing their entropy, and decreasing the system's free energy.

To quantitatively test the AO model, we fit the low concentration data (after subtracting the weak attraction of the $\phi_S = 0$ curve) with a modified AO form:

$$F_{AO}(r) = \frac{k_B T \phi_S^*}{(2a_S^*)^3} (2a_S^* + 2a_L - r)^2 \times \left(2a_S^* + 2a_L + \frac{r}{2} \right), \quad (1)$$

where $a_S^* = a_S + \delta a_S$ and $\phi_S^* = \phi_S(1 + \delta a_S/a_S)^3$ are the effective small sphere radius and volume fraction corrected to include the typical small sphere electrostatic interaction range $2\delta a_S$, and where a_S, a_L are the small and large spheres' bare radii. We model the effect of our 15 nm instrumental resolution by first converting $F_{AO}(r)$ to a probability distribution $P(r)$ via the Boltzmann relation, then smoothing $P(r)$ with a Gaussian kernel with a half-width of 15 nm, and then finally converting $P(r)$ back to a potential by a natural logarithm. The curves shown in

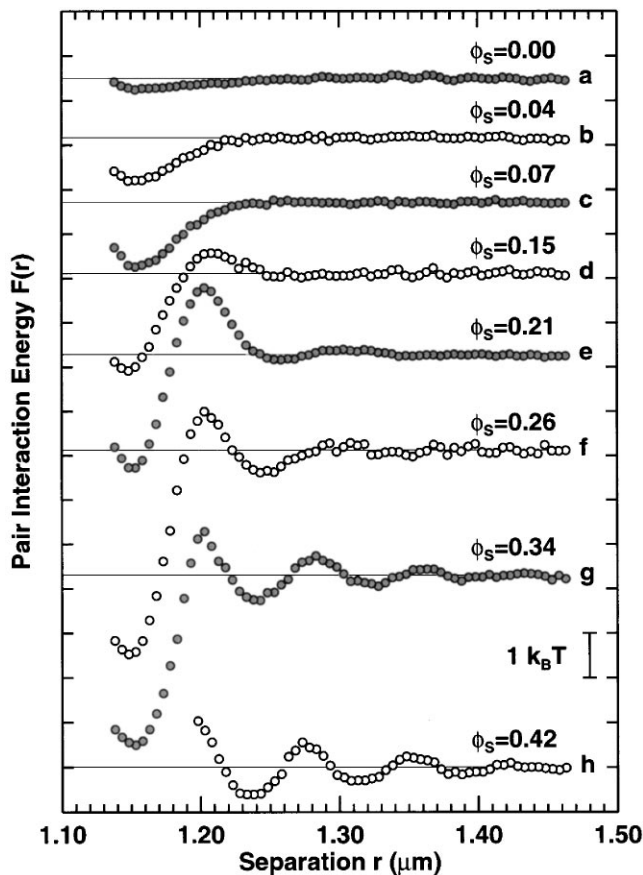


FIG. 1. The entropic interaction potentials measured with small sphere volume fractions ranging from $\phi_s = 0$ to 0.42 (the large sphere volume fraction was less than 10^{-7}). At the lowest volume fractions [curves (b), (c)] the potential is monotonically attractive, resembling the Asakura-Oosawa depletion model [1]. As more spheres are added, a repulsive barrier forms [(d), (e)], then a secondary minimum (f), before becoming fully oscillatory [(g), (h)]. The spheres for curve (h) never reached the primary depletion minimum. Each curve had to be shifted [16] a small amount horizontally to register their primary minima, due to the roughly 15 nm sphere polydispersity. The weak attraction seen in the $\phi_s = 0$ case is presumably due to van der Waals attraction [17,18].

Fig. 3 are typical fits with $\delta a_S = 7 \pm 3$ nm and a_L taken as free parameters. Models with $\delta a_S = 0$ typically underestimate the well depth by 30%–50%.

Our measurements also convincingly show that, when $\phi_s > 0.1$, there is a substantial depletion *repulsion* [3] at separations of about one small sphere diameter from contact. This repulsion, which is not predicted by the AO model, can be qualitatively explained by realizing that the small spheres will tend to form layers around the large spheres (Fig. 2b). When the gap between the spheres is commensurate with these layers, the free energy is lower; when incommensurate, the energy is higher. For $\phi_s \geq 0.25$, the effect of the higher order shells becomes significant, making the potential oscillatory (Fig. 1). The oscillation wavelength decreases monotonically as the concentration is increased, and is comparable to the mean

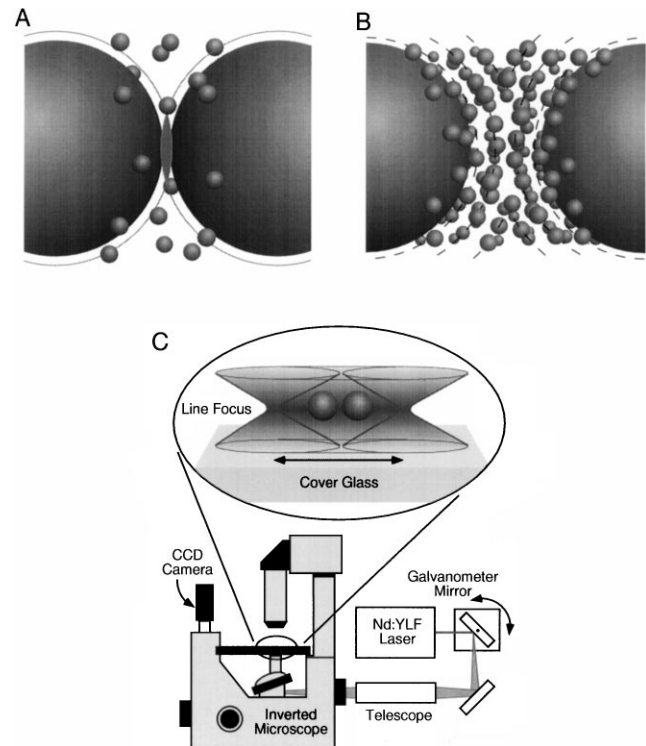


FIG. 2. (a) Each large sphere is surrounded by a “depletion zone” whose thickness equals the small sphere radius, indicated by the gray line, into which the centers of the small spheres cannot penetrate. The lens-shaped overlap region (shaded) results in a net increase in the volume available to the small spheres, increasing their entropy and producing a net attraction. (b) At higher volume fraction, the small spheres’ liquid structure leads to the formation of shells around the large spheres, analogous to fluid layering near a flat wall. The resulting entropic interaction has an oscillatory form. (c) A schematic diagram of the line optical tweezer apparatus. A galvanometer mirror scans an IR laser, coupled by a Keplerian telescope into a Zeiss Axiovert 135 microscope. The focus scans a roughly 10 μm line in the focal plane at 180 Hz.

spacing in the small sphere fluid, in qualitative agreement with recent calculations by Dickman *et al.* [3].

In addition to information regarding the two spheres’ energetics, our measurements also provide dynamical information. The most interesting feature we observe is a dramatic slowing of the two spheres’ relative Brownian motion as ϕ_s was increased. Briefly, we counted the number of times the two large spheres thermally activated into the primary depletion minimum during each one hour measurement. For the $\phi_s = 0.21$ run, the beads came together more than 200 times, and for the $\phi_s = 0.34$ case, only 3 times. Since the corresponding depletion repulsion barriers are superficially the same and the measured large sphere diffusivities are within a factor of 2, this slowing is completely unexpected.

To fall into the primary minimum, the large spheres must first squeeze out the dense monolayer of small spheres between them. It seems likely that the anomalous slowing could be due to the peculiar hydrodynamics,

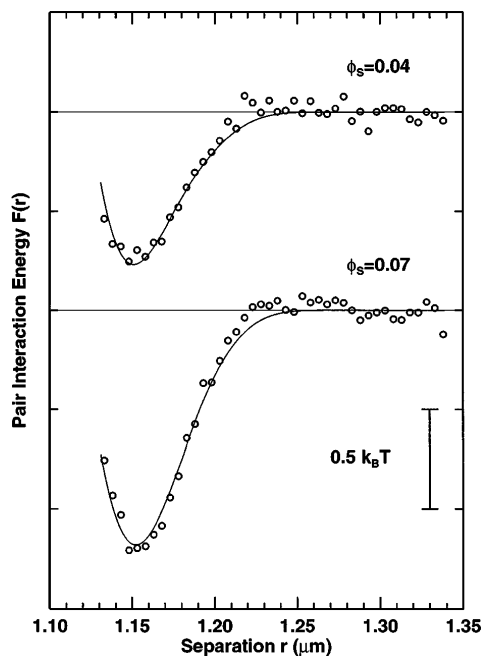


FIG. 3. Data for $\phi_S = 0.04$ and $\phi_S = 0.07$ with the background potential ($\phi_S = 0$) subtracted. The upturn on the left-most end of the curves is due to the resolution broadened bare repulsion [13,17] of the two large spheres. The curves are fits to the Asakura-Oosawa model, Eq. (1), blurred with a Gaussian kernel to account for our instrumental resolution.

phase behavior, or collective motion of that quasi-two-dimensional layer. It is also possible that there exists a very high (and very narrow) energetic barrier which merely appears small due to our finite resolution. Understanding this barrier will likely require new theoretical insight, perhaps by simulations which include particle dynamics, unlike the earlier work [3].

Whatever their exact cause, our observations suggest that it may be possible to “entropically stabilize” colloids, which would otherwise aggregate, simply by adding an inert smaller species. Similar effects might significantly slow reaction rates in crowded macromolecular solutions, and introduce a multitude of metastable states in depletion-induced colloidal crystals. It also seems likely that the smaller than expected energy scales seen in earlier depletion experiments [6] carried out at large ϕ_S could be explained if this effect allowed the spheres to probe only the higher order, and thus weaker minima.

These data were collected with the microscope and optical tweezer system represented schematically in Fig. 2c. Optical tweezers exploit optical gradient forces to trap dielectric particles in three dimensions near the waist of a strongly focused laser beam [14]. We scan the laser focus from side to side, rapidly enough that a particle cannot follow the trap but responds instead to the time-averaged optical field. A pair of trapped spheres will then undergo Brownian diffusion along the line, while strongly confined in the two perpendicular directions [15]. They act as if threaded on a frictionless rod. Two properties of the line

tweezer are essential to our potential measurement. First, the tweezer-induced forces along the line of the sphere centers are weak enough to be easily subtracted from the measured free energy. Second, the tweezer serves to strongly confine both spheres to the microscope’s focal plane, allowing us to equate the in-plane separation measured from a video image and the spheres’ actual three-dimensional separation.

We seal about 20 μl of the binary suspension between a microscope slide and cover glass with a 120 μm thick Parafilm spacer. We then trap a single pair of 1.1 μm PMMA spheres on the line focus, about 1.5 μm above contact with the cover glass. Control measurements indicate no wall-induced effects at this separation—more than 400 screening lengths or 15 small bead diameters. This distance also gives the best optical trapping and thus spatial resolution for the measured potential. We typically videotape the two spheres for one hour, which yields 2×10^5 separation measurements.

Accurately measuring the separation of the two spheres was complicated by the overlap of their diffraction-broadened images. On top of the roughly 15 nm random error caused by camera noise and the small out of plane motion, overlap effects cause a systematic overestimation of the sphere separation. At contact, the apparent distance between the two image centroids [19] was typically 100 nm larger than the actual center-center separation. We applied a correction procedure which assumes that the individual sphere images overlap via linear superposition of brightness. For instance, when finding the centroid of the right sphere, we must first subtract the contribution of the left sphere from the image. We used a mirror-reversed copy of the left sphere’s isolated left-hand side as a model for its overlapping right-hand side. We estimate that the residual overlap error is less than 30 nm at contact, and the resulting spatial warping of our data to be less than 10%.

The optical tweezer induces two types of forces on the spheres, which were subtracted from the data using the procedure shown in Fig. 4. If the scan rate of the tweezer is not completely uniform, the particles will migrate along the line to regions where the scan rate is slowest (i.e., where the time-averaged electric field is greatest). We used a nonuniform scan waveform such that the two spheres shared a one-dimensional, roughly harmonic potential well. This external force field speeds data collection for small separations and causes the fictitious attraction observed at long range. At slow scan rates, the tweezer can “kick” the beads [15] in the scan direction. For our fast bidirectional scanning any small kicks cancel each other, leaving unbiased Brownian motion.

We also observe and correct for a gentle repulsion at intermediate distance, indicated in Fig. 4. This repulsion is present even when $\phi_S = 0$. Its strength depends on both the laser power and polarization, and its range is comparable to the width of our laser focus. This repulsion is likely caused by the dipole-dipole interaction [20]

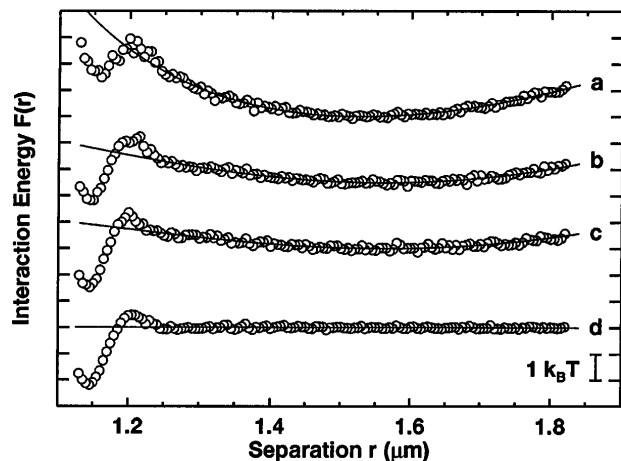


FIG. 4. Curves (a)–(c) show typical interaction potentials measured at three laser powers, 140 mW (a), 100 mW (b), and 70 mW (c). The gentle curvature of the potentials is due to tweezer-induced forces. The short-range attraction at the leftmost end of the curves is due to depletion ($\phi_S = 0.15$). To isolate the depletion interaction, we fit potentials measured at six different powers beyond $1.25 \mu\text{m}$ with a smooth function (a quadratic plus an exponential) and subtracted the fit. The resulting curves were mutually consistent to within statistical errors. This confirms that our fits accurately modeled the laser-induced potentials and that the depletion interaction itself is not significantly perturbed by our laser trap. Curve (d) shows the average of six such corrected potentials.

between the optical-frequency electric dipole moments induced when both spheres are in the laser focus.

Our measurements of depletion forces and kinetics provide detailed information about the structure and rheology of the background suspension—in this case details that are too small to be studied with ordinary microscopy or light scattering. In addition to the monodisperse hard spheres used in this study, we can measure the depletion effects due to soft polymer coils [7,11], rodlike colloids, or polydisperse spheres. Such research should provide substantial insight into the properties of these interesting suspensions as well as their biological analogs.

We thank P.D. Kaplan, D. Weitz, T.C. Lubensky, R. Verma, R. Kamien, and E. Hobbie for enlightening discussions. This work was supported by the U.S. NSF Grant No. DMR 96-23441 and the PENN Materials Research Laboratory, Grant No. DMR 96-32598.

*Present address: Center for Bio/Molecular Science and Engineering, Naval Research Lab, Washington, DC 20375.

- [1] S. Asakura and F. Oosawa, *J. Polym. Sci.* **33**, 183 (1958).
- [2] A. Vrij, *Pure Appl. Chem.* **48**, 471 (1976).
- [3] R. Dickman, P. Attard, and V. Simonian, *J. Chem. Phys.* **107**, 205 (1997); B. Götzmann, R. Evans, and

- S. Deitrich, *Phys. Rev. E* **57**, 6785 (1998); X.L. Chu, A.D. Nikolov, and D.T. Wasan, *Langmuir* **12**, 5004 (1996); T. Biben, P. Bladon, and D. Frenkel, *J. Phys. Condens. Matter* **8**, 10799 (1996); J. Piasecki, L. Bocquet, and J.P. Hansen, *Physica (Amsterdam)* **218A**, 125 (1995); Y. Mao, P. Bladon, H.N.W. Lekkerkerker, and M.E. Cates, *Mol. Phys.* **92**, 151 (1997).
- [4] W.C.K. Poon and P.B. Warren, *Europhys. Lett.* **28**, 513 (1994).
- [5] P.D. Kaplan, J.L. Rouke, A.G. Yodh, and D.J. Pine, *Phys. Rev. Lett.* **72**, 582 (1994); A.D. Dinsmore, A.G. Yodh, and D.J. Pine, *Phys. Rev. E* **52**, 4045 (1995).
- [6] P.D. Kaplan, L.P. Faucheux, and A.J. Libchaber, *Phys. Rev. Lett.* **73**, 2793 (1994); A.D. Dinsmore, A.G. Yodh, and D.J. Pine, *Nature (London)* **383**, 239 (1996).
- [7] D.L. Sober and J.Y. Walz, *Langmuir* **11**, 2352 (1995); A. Sharma and J.Y. Walz, *J. Chem. Soc. Faraday Trans.* **92**, 4997 (1996); A. Milling and S. Biggs, *J. Colloid Interface Sci.* **170**, 604 (1995).
- [8] P. Richetti and P. Kekicheff, *Phys. Rev. Lett.* **68**, 1951 (1992); J.L. Parker, P. Richetti, P. Kekicheff, and S. Sarman, *Phys. Rev. Lett.* **68**, 1955 (1992).
- [9] Y.N. Ohshima *et al.*, *Phys. Rev. Lett.* **78**, 3963 (1997).
- [10] O. Mondain-Monval, F. Leal-Calderon, F. Phillip, and J. Bibette, *Phys. Rev. Lett.* **75**, 3364 (1995).
- [11] R. Verma, J.C. Crocker, T.C. Lubensky, and A.G. Yodh, *Phys. Rev. Lett.* **81**, 4004 (1998).
- [12] The weight fraction of small spheres ϕ_w in each sample was determined by weighing the dried sample. This was then converted to a volume fraction ϕ_S by $\phi_S = (1.28 \pm 0.04)\phi_w$. The factor 1.28 was determined by measuring the viscosity of dilute small sphere suspensions and fitting the data to $\nu = \nu_0(1 + 2.5\phi_S)$, and accounts for any small sphere porosity and swelling in contact with water.
- [13] J.C. Crocker and D.G. Grier, *Phys. Rev. Lett.* **77**, 1897 (1996).
- [14] A. Ashkin, J.M. Dziedzic, J.E. Bjorkholm, and S. Chu, *Opt. Lett.* **11**, 288 (1986); R.S. Afzal and E.B. Treacy, *Rev. Sci. Instrum.* **63**, 2157 (1992).
- [15] L.P. Faucheux, L.S. Bourdieu, P.D. Kaplan, and A.J. Libchaber, *Phys. Rev. Lett.* **74**, 1504 (1995); L.P. Faucheux, G. Stolovitzky, and A.J. Libchaber, *Phys. Rev. E* **51**, 5239 (1995).
- [16] The contact separation used to shift Fig. 1, curve (h), was found by forcing the two spheres into the primary minimum (not shown) using the laser tweezer. Since for curve (g) the spheres explored only the primary minimum 3 times during the one hour experiment, the depth of the minimum could be roughly $1k_B T$ in error.
- [17] W.B. Russel, D.A. Saville, and W.R. Schowalter, *Colloidal Dispersions* (Cambridge University Press, Cambridge, 1989).
- [18] T. Sugimoto, T. Takahashi, H. Itoh, S. Sato, and A. Muramatsu, *Langmuir* **13**, 5528 (1997).
- [19] J.C. Crocker and D.G. Grier, *J. Colloid Interface Sci.* **179**, 298 (1996).
- [20] M.M. Burns, J.M. Fournier, and J.A. Golovchenko, *Phys. Rev. Lett.* **63**, 1233 (1989); M.M. Burns, J.M. Fournier, and J.A. Golovchenko, *Science* **249**, 749–754 (1990).